

Supercontinuum generation with superior intrapulse coherence in dispersion-tailored waveguides

Chao Mei

Max Born Institute for Nonlinear Optics and Short Pulse Spectroscopy, Max-Born-Straße 2a, 12489 Berlin, Germany
chao.mei@mbi-berlin.de

Günter Steinmeyer

¹Max Born Institute for Nonlinear Optics and Short Pulse Spectroscopy, Max-Born-Straße 2a, 12489 Berlin, Germany

²Institut für Physik, Humboldt Universität zu Berlin, Newtonstraße 15, 12489 Berlin, Germany
steinmeyer@mbi-berlin.de

Abstract—Intrapulse coherence is an important performance metric for applications of supercontinua, including precision frequency metrology and attosecond science. These applications require a stable carrier-envelope phase, which is usually measured by f - $2f$ interferometry. Here, the potential for superior intrapulse coherence with 100 and 400-fs input pulses is studied, exploiting different dispersion profiles. The simulation results in this study provide a guideline for coherent spectral broadening, which can be exploited to minimize fluctuations of the carrier-envelope phase.

Index Terms—supercontinuum, coherence, dispersion, waveguide

The stabilization of the carrier-envelope phase is highly important for high-field physics, the generation of isolated attosecond pulses, and precision frequency metrology [1]. Most stabilization schemes are based on f - $2f$ interferometry, in which an octave-spanning supercontinuum (SC) is required [2]. Such a broadband spectrum can only be generated extracavity, given the limited energy inside the laser cavity. In terms of SC broadening, best performance is typically achieved by launching the input spectrum near the zero-dispersion wavelength (ZDW) of the fiber. When the nonlinearly broadened spectrum extends into the anomalous dispersion region and forms a soliton, the pulse quickly reaches a high soliton order and decays into several fundamental solitons, as second-order dispersion is low near the ZDW. Here, modulation instability comes into play, effectively providing gain for noise amplification. Consequently, the broadening efficiency of the SC comes at the high price of a pronounced susceptibility towards noise on the input pulse train [3]. As a result, the coherence of the pulse train may severely degrade, i.e., pulses in the pulse train cannot be compressed with identical phases, given their fluctuations both in amplitude and phase.

While pulse-to-pulse coherence has been extensively discussed in literature [4], much less attention has been paid to intrapulse coherence, despite its critical role for many applications. The difference between these two coherence types is that the pulse-to-pulse coherence is about the phase correlation between the pulses at a different time while the

intrapulse coherence is about the phase correlation between the spectral components at different frequencies. One therefore needs carefully distinguish these two types of coherence.

In the following, we investigate four kinds of dispersion profiles in Ge-doped four-layer silica fibers with cylindrical symmetry. In particular, two typical dispersion profiles exhibiting two ZWDs and all-normal dispersion (ANDi) are appear exceptionally promising for coherent SC generation. In our study, we use a generalized nonlinear envelope equation rather than the conventionally used generalized nonlinear Schrödinger equation to avoid limitations from the slow-varying envelope approximation [5]. As input noise strongly influences the resulting coherence performance, we use a newly developed analytical model [6] to describe the additive noise induced by amplified simultaneous emission in a laser cavity. Furthermore, we couple the spontaneous Raman emission into the propagation equation as a stochastic Langevin source term.

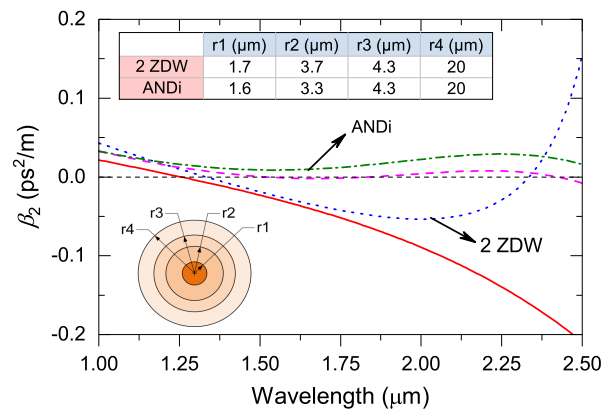


Fig. 1. Different designed dispersion profiles of the proposed Ge-doped four-layer cylindrical silica fibers.

The dispersion profiles are designed by changing the geometrical dimensions of r_1 , r_2 , r_3 , and r_4 as well as the corresponding refractive indices n_1 , n_2 , n_3 , and n_4 . The number of ZWDs and the value of group-velocity dispersion can be adjusted accordingly. Here we chose values for a

profile with 2 zero-dispersion wavelengths (2-ZDW) and an all-normally dispersive profile (ANDi). Corresponding values of n_1 to n_4 for the two profiles are 1, 0.2, 0.8, and 0.6 and 0.6, 0.2, 0.3, and 0.2, respectively.

Generated SC, resulting pulse-to-pulse coherence (g_{12}) and intrapulse coherence (Γ) after 10-cm propagation are shown in Fig. 2. Here a pump wavelength of $1.55 \mu\text{m}$ was assumed. The injected peak powers for 2-ZDW and ANDi profiles are 30 and 200 kW, respectively. While all spectra in Fig. 2(a) encompass more than one octave, the coherence properties are quite different. For the 2 ZDW profile, the values of g_{12} for the 100-fs pulse approach unity in the wavelength range of interest while for the 400-fs pulses, most values are below 0.25, except for a narrow-band range around $1.6 \mu\text{m}$, which relates to a heavily damped $2f$ component at $3.2 \mu\text{m}$, which appears of little practical relevance. In contrast, for the ANDi profile, the values of g_{12} approach unity for both, 100 and 400-fs input pulses from $1.9 \mu\text{m}$ to $2.5 \mu\text{m}$, as shown in Fig. 2(b). This feat is caused by the absence of the modulation instability in the ANDi region. Therefore, noise amplification is greatly suppressed during the spectrum broadening. In Fig. 2(c), intrapulse coherence manifests itself in a different manner compared to the pulse-to-pulse coherence. At $1.6 \mu\text{m}$ wavelength, Γ suddenly drops below 0.25 for the 2 ZDW profile when the input width is 100 fs. This means that spectral components larger than $3.2 \mu\text{m}$ have rather unstable phases. For the 400-fs input, instead, the situation is even worse, as intrapulse coherence is vanishing throughout the entire spectrum. In contrast, the values of Γ for ANDi profile are nearly 1 in a much broader range because noise amplification induced by the modulation instability is nearly completely mitigated.

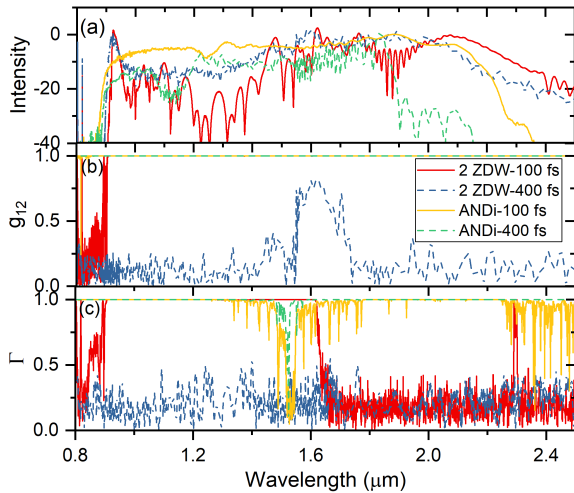


Fig. 2. Resulting (a) SC, (b) pulse-to-pulse coherence and (c) intrapulse coherence for the 2-ZDW profile for 100-fs input pulses (red solid curves) and 400-fs input pulses (blue dashed curves). In addition, curves are shown for the ANDi profile (100-fs input, yellow solid curves) and 400-fs input (green dashed curves). Pump wavelength for all cases was assumed as $1.55 \mu\text{m}$

We further ran numerical simulations to clarify the break-up of coherence with propagation distance z . As can be seen

from Fig. 3(a), intrapulse coherence quickly approaches unity within 2 cm, when the input width is 100 fs. In contrast, when the pulse width is increased to 400 fs, intrapulse coherence significantly degrades at similar length scales. This means longer pulse is rather unsuitable for obtaining high intrapulse coherence with a 2-ZDW profile. However, resultant patterns for ANDi profile appear much more promising, regardless of whether the input duration is 100 or 400 fs. In particular, the coherent bandwidth occupied by high intrapulse coherence is much broader. Moreover, intrapulse coherence already reaches its maximum value within much shorter propagation, e.g., when the input width is 100 fs. We therefore conclude that ANDi profiles exhibit an obvious edge compared to rather conventional 2-ZDW profiles, which pay out in a high intrapulse coherence. Nevertheless, this edge does not come without a price to pay, i.e., significantly higher input peak powers are required to warrant this apparent advantage in terms of coherence.

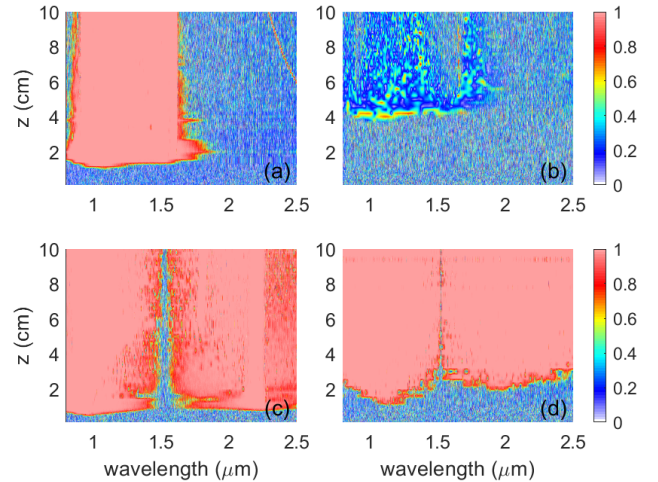


Fig. 3. Evolution of intrapulse coherence along propagation under the conditions of (a) 2-ZDW with 100 fs duration, (b) 2-ZDW with 400 fs duration, (c) ANDi with 100 fs duration, and (d) ANDi with 400 fs duration

REFERENCES

- [1] E. Goulielmakis, E. Uiberacker, R. Kienberger, A. Baltuska, V. Yakovlev *et al.*, “Direct measurement of light waves,” *Science*, vol. 305, pp. 1267–1269, Aug. 2004.
- [2] H. R. Telle, G. Steinmeyer, A. E. Dunlop, J. Stenger, D. H. Sutter *et al.*, “Carrier-envelope offset phase control: a novel concept for absolute optical frequency measurement and ultrashort pulse generation,” *Appl. Phys. B*, vol. 69, pp. 327–332, Feb. 1999.
- [3] J. M. Dudley, G. Genty, and S. Coen, “Supercontinuum generation in photonic crystal fiber,” *Rev. Mod. Phys.*, vol. 78, pp. 1135–1184, Oct. 2006.
- [4] Y. Zhang, J. Kainerstorfer, J. C. Knight, and F. G. Omenetto, “Experimental measurement of supercontinuum coherence in highly nonlinear soft-glass photonic crystal fibers,” *Opt. Express*, vol. 25, pp. 11 842–11 852, Aug. 2017.
- [5] G. Genty, P. Kinsler, B. Kibler, and J. Dudley, “Nonlinear envelope equation modeling of sub-cycle dynamics and harmonic generation in nonlinear waveguides,” *Opt. Express*, vol. 15, pp. 5382–5387, Apr. 2007.
- [6] R. Liao, C. Mei, Y. Song, A. Demircan, and G. Steinmeyer, “Spontaneous emission noise in mode-locked lasers and frequency combs,” *Phys. Rev. A*, vol. 102, pp. 013 506–1–12, Jul. 2020.